ELSEVIER

Journal of Nuclear Materials 306 (2002) 194–201

journal of nuclear materials

www.elsevier.com/locate/jnucmat

Study of the thermoelectric power evolution of Zr-based alloys with Nb additions

Seon Jin Kim, Hyun Seon Hong *, Young Min Oh

Division of Materials Science and Engineering, Hanyang University, Seoul 133-791, South Korea

Received 3 July 2002; accepted 21 September 2002

Abstract

The thermoelectric power (TEP) evolution of zirconium alloys was investigated by varying the niobium content from 0.1 to 0.8 at.%. The phase-transformation temperature and the recrystallization behavior of the alloys were characterized by the TEP evolution from 550 to 940 °C, which showed that the α to β phase-transformation temperature decreased as the Nb content increased. The phase transformation occurred in the temperature range 910–940 °C for the 0.2 at.% Nb addition while the transformation occurred below 850 °C for the 0.8 at.% Nb addition. For the 0.2 at.% Nb addition, the aging time required for the completion of recrystallization was about 60 min in the temperature range of 575–600 °C and about 10 min in the range of 625–650 °C. However, as the Nb addition increased to 0.5 at.%, the required aging time for the recrystallization turned out to be longer than the 0.2 at.% Nb addition. In addition, an equation for the solution limit of niobium for the present specimens was established from the experimental results and microstructural characteristics of TEP were discussed.

1. Introduction

Zirconium alloys have been widely used as a cladding material in pressurized water reactors. However, the trend to extended cycle lengths with high coolant lithium level has led to an increased demand on the oxidation resistance and the mechanical property of the cladding material. Recently, many studies have been done to improve the mechanical property and corrosion resistance by changing the chemical composition of cladding materials and by optimizing heat-treatment processes [1–3]. Corrosion properties are reported to be fairly dependent on the themomechanical treatment during the fabrication process. Therefore, the study of the microstructural characteristics such as recrystallization behavior and the solution limit of alloying elements is indispensable for the optimum fabrication of nuclear fuel claddings.

In order to study the solid solution limit of alloying elements, some experimental techniques including microstructural observations, lattice parameter calculations and resistance measurements [4–10] as well as a theoretical analysis of thermodynamics [11] have been used. The thermoelectric power (TEP), based on the Seebeck effect, is associated with the flux of electrons when the material is subjected to an electrochemical potential gradient or to a temperature gradient. TEP is a function of microstructural parameters such as texture and work hardening as well as temperature. Thus, it is possible to determine the solution limit of an alloying element by modifying the TEP variation to be dependent only on the concentration of a solute in the solid solution. It is also possible to evaluate the recrystallization behavior of the cold-rolled specimens for a given composition [12–15]. Recently, it was reported that the solution limit of iron in zirconium-base alloys was determined exactly by TEP measurements, which are a useful and practical technique for the evolution of

* Corresponding author. Tel.: +82-2 2290 0382; fax: +82-2 2281 4914.

E-mail address: hshong@ihanyang.ac.kr (H.S. Hong).

0022-3115/02/$ - see front matter
PII: S0022-3115(02)01260-6

the solid solution during isothermal heat treatments. Studies on the microstructural evolution of aluminum-base alloys by TEP measurements were also reported [16,17].

In this study, the solution limit of niobium was evaluated by TEP measurements in a zirconium–0.8 at.% tin alloy, which is the nominal composition of advanced zirconium-base alloys for nuclear fuel claddings [18]. The phase transformation and recrystallization of the zirconium-base alloys were also investigated by TEP measurements by varying the microstructural parameters.

2. Experimental procedure

Six button-type ingots of zirconium alloys were prepared from high purity sheet-type zirconium and alloying elements by arc melting. The niobium content was varied from 0.1 to 0.8 at.% while the tin content was fixed at 0.8 at.%. The alloys were re-melted five times for homogenization. The quantity of impurities in these alloys was rarely changed from that in pure zirconium from Cezus, and the chemical compositions of the alloys are given in Table 1. The ingots were solution-treated at 1050 °C for 20 min under vacuum and then water-quenched. The quenched ingots were fabricated into sheet-type by the processes of hot rolling, cold rolling and annealing at 610 °C for 2 h. The testing specimens with the dimension of 50 mm (L) × 8 mm (W) × 1 mm (t) were obtained from the sheets.

To avoid a texture evolution during homogenization treatment, the specimens were pre-annealed at 850 °C for 12 h in a vacuum furnace. After the pre-annealing, successive heat treatments were carried at 30 °C increments from 550 to 940 °C on the same specimen, and the specimens were water-quenched at the end of each homogenization step. The specimens were held at each temperature for 30 min. It was reported that it takes only a few minutes to reach the equilibrium concentration of alloying element at 600 °C [13].

The TEP of the specimens interrupted by water-quenching after the homogenization treatment had been measured at ambient temperature ($T = (15 \pm 0.1)$ °C, $\Delta T = (10 \pm 0.1)$ °C) under vacuum. Two blocks made with a reference metal are maintained at temperature T and $T + \Delta T$, respectively. Copper was used for a reference metal. Both ends of the flat specimen were pressed with the reference blocks so as to ensure good thermal and electrical contact. The specimen-reference block contact was secured by clamping it down with screws. It is well known that the Seebeck voltage is developed in a closed circuit made of two metals when the two junctions are maintained at different temperatures. The principle of TEP is to measure the voltage change (ΔV) produced by the Seebeck effect between the specimen and two metallic reference blocks at temperatures T and $T + \Delta T$. The relative thermoelectric power $\Delta S(= \Delta V/\Delta T)$ was obtained by dividing the difference in potential (ΔV) associated with both the variation of the electrochemical potential and the change in the electronic distribution by the temperature difference (ΔT).

To investigate the effect of the recovery and recrystallization on TEP, the cold-rolled zirconium–0.8 at.%Sn alloys of different niobium concentrations were annealed in the temperature range of 575–650 °C. The TEP of the specimens interrupted by water quenching was measured in the same manner described previously. Due to the complexity of microstructural evolutions in the electronic structure, it was difficult to identify a particular microstructural evolution by the TEP variation. Complementary observation techniques of hardness measurement and optical and electron microscopy were carried out. The hardness of the water-quenched specimens was measured with a Vickers microhardness testing equipment under the load of 200 g. Prior to optical microscopy, specimens were mechanically polished and etched using a solution composed of 5 vol.% HF, 45 vol.% HNO_3 and 50 vol.% distilled H_2O. Thin foils for transmission electron microscopy were prepared from the middle part of the specimens by mechanically thinning to about 100 m thickness. Discs, 3 mm in diameter, were punched out of these 100-m thin foils and then electropolished. Electropolishing was done in a solution of 90 vol.% ethanol + 10 vol.% perchloric acid at below −40 °C.

Table 1
Chemical composition of zirconium-alloys (at.%)

Alloys	Zr[a]	Nb		Sn	
		Nominal	ICP analysis	Nominal	ICP analysis
Alloy-1	Bal.	0.1	0.13	0.8	0.75
Alloy-2	Bal.	0.2	0.23	0.8	0.76
Alloy-3	Bal.	0.3	0.33	0.8	0.75
Alloy-4	Bal.	0.5	0.51	0.8	0.76
Alloy-5	Bal.	0.8	0.76	0.8	0.76

[a] The total amount of Fe, Cr and Ni were analyzed to be less than 0.01 at.%.

3. Results and discussion

Fig. 1 shows the TEP evolutions of Alloy-1, Alloy-3 and Alloy-5 as a function of the homogenization temperature. In the case of Alloy-1, a little variation in TEP was observed as the homogenization temperature increased from 570 to 650 °C. However, the TEP decreased in the temperature range 650–700 °C. The saturation of TEP was found between 700 and 760 °C. For Alloy-3, a rapid decrease in TEP occurred in the temperature range 670–730 °C, followed by a saturation of the TEP between 730 and 760 °C. The TEP evolution for Alloy-5, containing the highest niobium concentration, showed a continuous decrease in TEP up to 800 °C without saturation corresponding to the complete dissolution of niobium in the matrix.

Fig. 2 shows the optical microstructure of the homogenized Alloy-1 at 700 and 760 °C. Precipitates were easily observed on the grain boundaries at the homogenization temperatures of 580 and 640 °C where little variation in TEP was observed. However, precipitates were not found in the specimens homogenized above 700 °C as shown in Fig. 2, indicating the saturation of TEP. Fig. 3 shows the optical micrographs of Alloy-3 homogenized at the same temperatures used for Alloy-1. Precipitates were observed in the specimens homogenized at 580, 640 and 700 °C. It should be noted that precipitates were not present in Alloy-1 at 700 °C. This difference seems to cause the retarded saturation of the TEP in Alloy-3 from 700 to 730 °C compared to Alloy-1. The microstructural study of Alloy-5 showed that precipitates were not found in any specimen homogenized at 580, 640, 700 and 760 °C, however, the second phase around the grains could be seen in specimens homogenized below 700 °C. This phase disappeared at the homogenization temperature of 760 °C, which is above the eutectoid temperature. Thus, the continuous decrease of TEP for Alloy-5 might be explained by the presence of the β-phase without passing the α-domain during homogenization.

The absolute thermoelectric power of transition metals [19,20] can be written by

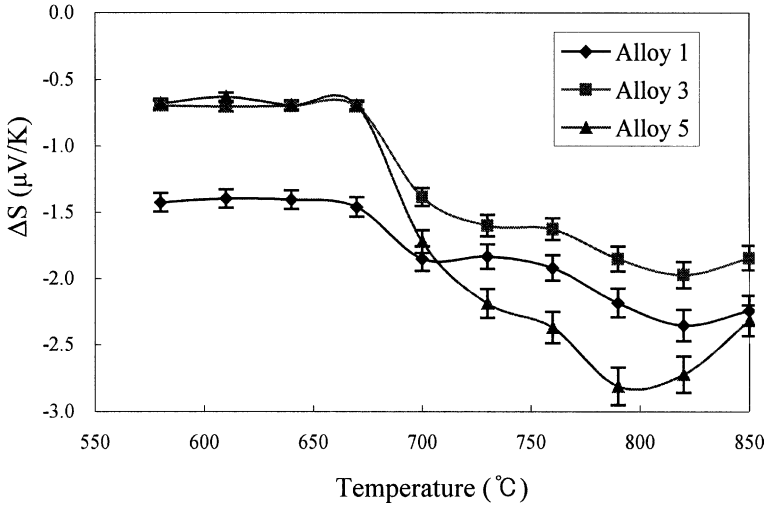

Fig. 1. TEP changes as a function of homogenization temperature for Alloy-1, 3 and 5.

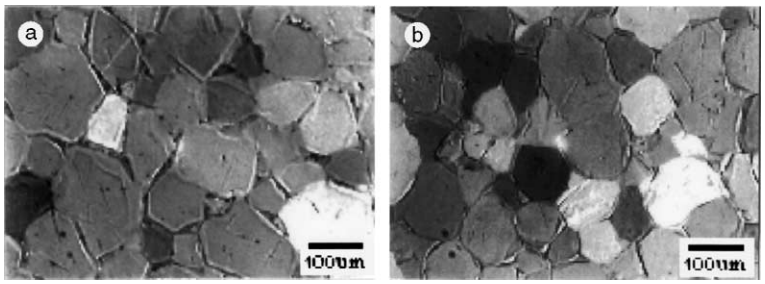

Fig. 2. Optical microstructure of Alloy-1 after the homogenization treatment at (a) 700 °C and (b) 760 °C.

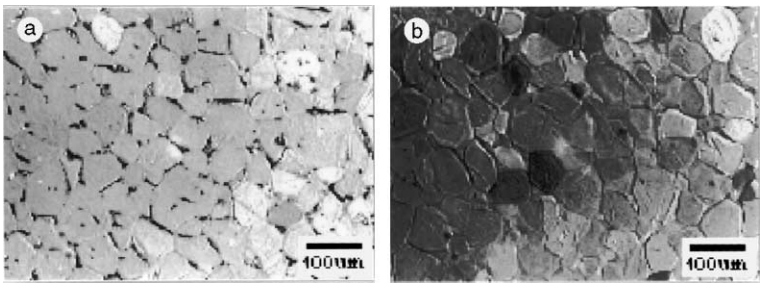

Fig. 3. Optical microstructure of Alloy-3 after the homogenization treatment at (a) 700 °C and (b) 760 °C.

$$S \approx -\frac{\pi^2}{2}\frac{k_B^2 T}{e(E_0 - E_F)}, \quad (1)$$

where k_B is the Boltzmann constant, T is the absolute temperature, e is the electron charge and E_0 and E_F are the energies of the top level of the d-band and of the Fermi level, respectively. Thus, $e(E_0 - E_F)$ represents the energy range of unoccupied states of the incompletely filled portion of the d-band. The valence electrons from the normal metal solute atoms tend to occupy hybridized d-level orbitals in the alloys of transition elements effectively decreasing the value of $(E_0 - E_F)$. The absolute thermoelectric power, consequently, becomes larger (more negative). The effects of a transition metal solute in the transition metals may be divided into two categories. The first category consists of those solute atoms with relatively large numbers of available d-orbitals, which causes the thermoelectric power to become smaller (less negative) by effectively increasing the value of $(E_0 - E_F)$. The other category of solutes may be represented by such elements whose d-levels are more filled. If the solute atom has fewer d-orbitals available than the solvent atom, it will decrease the value of $(E_0 - E_F)$ of the alloy causing the thermoelectric power to become larger (more negative). On the other hand, if the solute atom has more d-orbitals than the solvent atom, the value of $(E_0 - E_F)$ of the alloy will increase leading the thermoelectric power to be smaller (more positive) [19]. For example, in the case of the addition of niobium or iron in zirconium, the thermoelectric power of the alloy tends to become larger (more negative) because the solute atom has fewer d-orbitals available than the solvent atom and so the value of $(E_0 - E_F)$ decreases. Therefore, as the homogenization temperature increased, the TEP of the zirconium-base alloys decreased continuously until it was saturated. The saturation of TEP occurred only after the disappearance of the precipitates because all the solutes were dissolved in the matrix and did not affect the thermoelectric power.

The different TEP values after homogenization of the present specimens could be attributed to the small differences in impurity concentrations. The effect of the niobium content on the TEP evolution was investigated by normalization of the TEP values for all the specimens. The normalization was carried out using the relation, $\delta S_{Nb} = \Delta S_T - \Delta S_{550}$, where ΔS_T and ΔS_{550} were the TEPs of the specimens homogenized at the temperature T for 0.5 h and at 550 °C for 24 h, respectively. The curves obtained from the normalization were represented in Fig. 4. It can be seen that all the curves were superimposed at low temperatures below 670 °C, and the curves decreased in general above 670 °C, which could be attributed to the increase of the niobium content in the solid solution. When the TEP reaches a constant level corresponding to a complete solution of niobium in the α-domain, this niobium content is considered to be the solution limit at that temperature. Using Borrelly's method with the data obtained from the experiments [13], the solution limit of niobium in zirconium–0.8 at.% Sn alloy could be obtained by the following equation:

$$C_{Nb} = 4.69 \times 10^{10} \exp\left(\frac{-2.5 \times 10^4}{T}\right) \text{ (at.\%)}. \quad (2)$$

The solution limit of niobium in zirconium–0.8 at.% Sn alloy at the temperature of 730 °C was calculated to be 0.7 at.% by the above equation. The solution limit of niobium at 600 and 700 °C were 0.02, 0.33 at.%, respectively. The niobium addition in this alloy resulted in an increase of the eutectoid temperature, compared to the binary Zr–Nb alloy [21], and the solution limit of niobium decreased due to the tin addition.

To evaluate the presence of the β-phase on the TEP behavior in the zirconium-based alloys, the TEP variation (δS_{Nb}) was investigated as a function of the niobium content in the homogenization-temperature range 850–940 °C. As the homogenization temperature increased, the increase in the TEP of the specimens was observed in general as shown in Fig. 5. However, the saturation of the TEP was also observed for Alloy-3, -4 and -5 in the homogenization temperature range 880–910 °C. It is known that the phase-transition temperature can be determined by TEP measurements because the discontinuity occurred in the TEP when a phase is transformed. The employed homogenization temperatures in

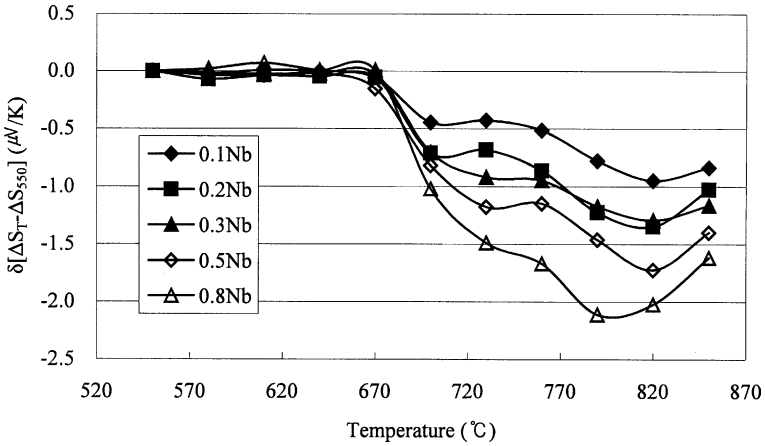

Fig. 4. $\delta[\Delta S_T - \Delta S_{550\ ^\circ C}]$ versus homogenization temperature for zirconium alloys.

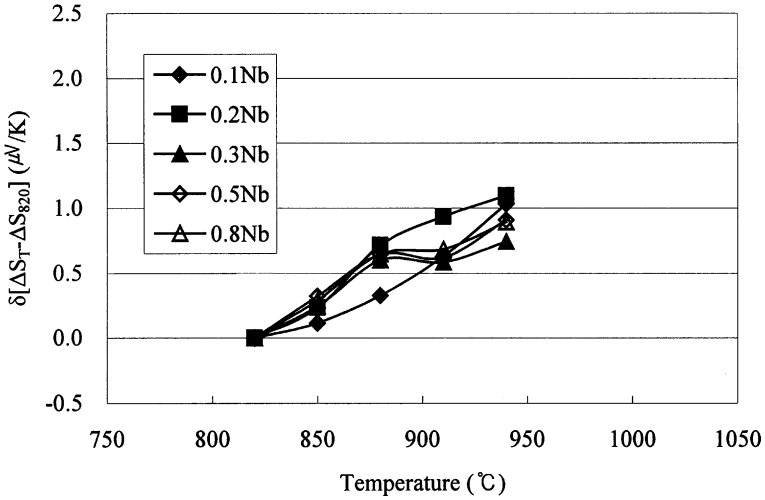

Fig. 5. $\delta[\Delta S_T - \Delta S_{820\ ^\circ C}]$ versus homogenization temperature for zirconium alloys.

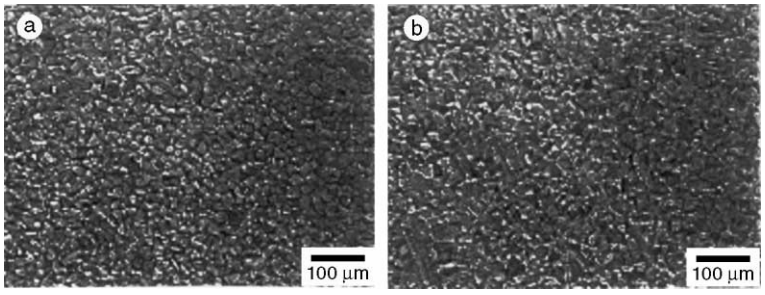

Fig. 6. Optical microstructure of Alloy-2 after the homogenization treatment at (a) 910 °C and (b) 940 °C.

this study were not the same as those at which TEP was measured, so it was difficult to apply the theory directly to the present results. However, it is reported that the β-quenched platelet-like structure is produced when quenched after annealing at high temperatures in the β-phase region. This fine platelet-like structure can act as a

dispersive center and an absorber of solute atoms due to its high solubility. Thus, the TEP of zirconium-base alloys will increase as the homogenization temperature increases. The optical microstructures of Alloy-2 and Alloy-5 were studied as a function of the homogenization temperature from 850 to 940 °C. Figs. 6 and 7 show

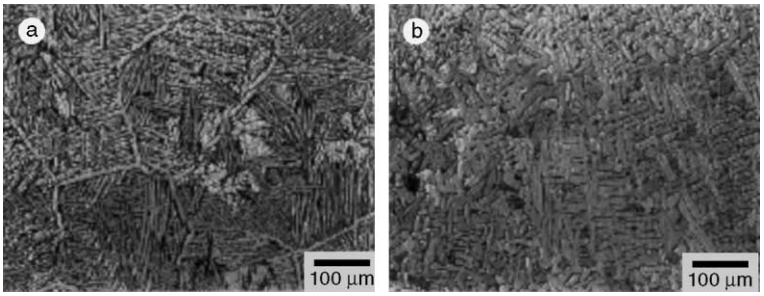

Fig. 7. Optical microstructure of Alloy-5 after the homogenization treatment at (a) 910 °C and (b) 940 °C.

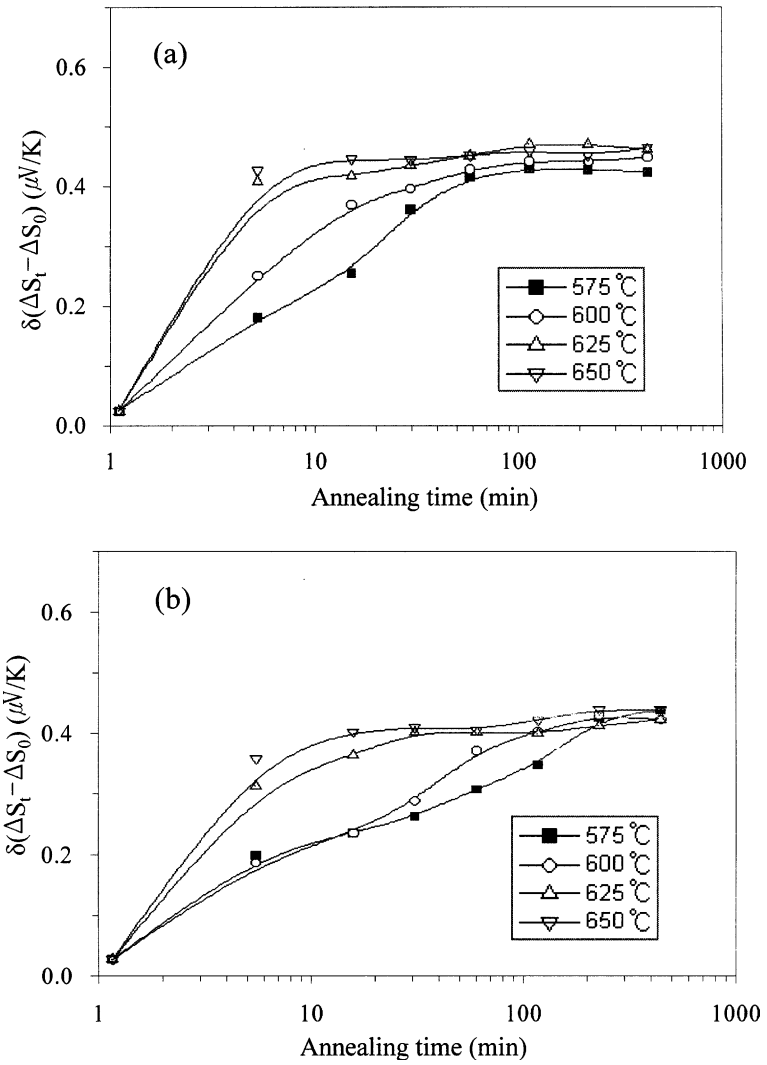

Fig. 8. Variations of $\delta S(=\Delta S_t - \Delta S_0)$ as a function of the aging time at various aging temperature for (a) Alloy-2 and (b) Alloy-4.

microstructures of Alloy-2 and Alloy-5 homogenized at 850 and 940 °C, respectively. In the case of Alloy-2, it can be seen that the microstructure was mainly composed of equiaxed α-grains but some portion of the α-grains transformed to a fine lath structure at 940 °C. For Alloy-5, the fine lath structure was observed at all temperatures. Consequently, from the investigation of the optical microstructure, it was considered that the phase transition from the α to β phase occurred between 910 and 940 °C for Alloy-2, and below 850 °C for Alloy-5.

The evolution of the TEP for the cold-rolled zirconium-base alloys, annealed for up to 480 min was investigated at 575 and at 650 °C, respectively. Fig. 8 shows the evolution of $\delta S(=\Delta S_t - \Delta S_0)$ as a function of the aging time at various aging temperatures for the specimens. ΔS_0 is the TEP of the cold-rolled zirconium-base alloy, and ΔS_t is the TEP of the cold-rolled zirconium alloy with aging for a period of time t. In all cases, the TEP started to increase at the early stage of the aging and reached a plateau, which is characteristic of a newly incubated phase [17]. In the early stage, the increase of the TEP was associated with the rearrangement of the dislocations and the extinction of the defects introduced by the cold rolling, and with the redistribution of solute atoms. The aging time required for reaching the plateau was about 60 min for Alloy-2 aged at 575 °C. At 650 °C, the aging time decreased to about 10 min. In the case of Alloy-4, the aging times for the plateau were 20 min at 575 °C and 240 min at 650 °C, respectively.

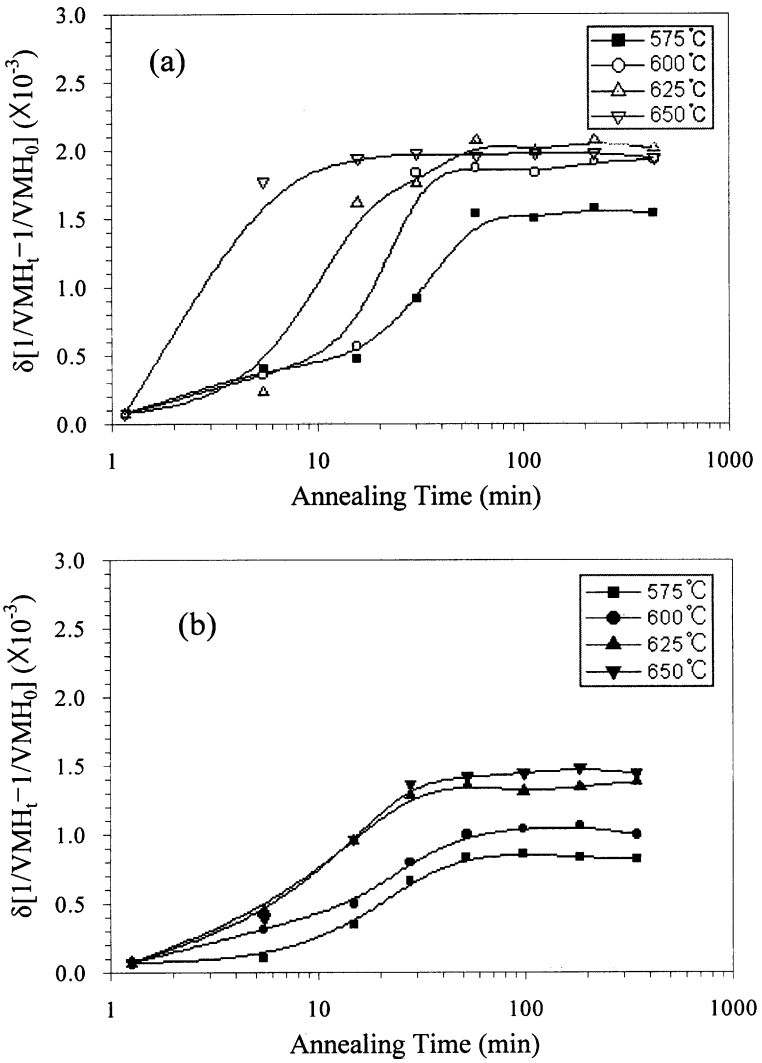

Fig. 9. Variations of $([1/VMH_T] - [1/VMH_0])$ as a function of the aging time at various aging temperature for (a) Alloy-2 and (b) Alloy-4.

Fig. 9 shows the Vickers microhardness (VMH) of Alloy-2 and Alloy-4. The hardness values were changed into the form of $([1/\mathrm{VMH}_T] - [1/\mathrm{VMH}_0])$, which are analogous to that of the TEP evolution, $(\Delta S_t - \Delta S_0)$, in order to study the behavior of recovery and recrystallization. The variation of hardness showed a similar trend to that of TEP evolution. However, the hardness slightly decreased in the early stage at the low aging temperatures, and the aging time for the plateau was shorter in the hardness evolution compared to the TEP evolution. The difference at the early stage resulted from the decrease in hardness during recrystallization. Considering the TEP and the hardness evolution, the recovery and recrystallization occurred almost at the same time before the completion of the recrystallization of zirconium-base alloys. In TEM micrographs of Alloy-4 aged at 600 °C for various aging times, it was found that even though the aging time increased the dislocations did not completely disappear, and thus the dislocation as well as the new grains were observed after aging for 60 min. The hardness evolution plateau did not correspond to the completion of the recrystallization of zirconium-base alloys for the same reason. Thus, the completion of the recrystallization of Alloy-2 required an aging time of about 60 min in the temperature range of 575–600 °C and about 10 min in the temperature range of 625–650 °C. In the case of Alloy-4, a longer aging time was required for the completion of recrystallization. Consequently, it was useful to determine the time required for the completion of the recrystallization by the analysis of the TEP evolution.

4. Conclusions

1. The thermoelectric power (TEP) of the zirconium-based alloys became larger (more negative) as the niobium additions increased. The reason for the negative increase in TEP is because niobium atoms have fewer d-orbitals than zirconium atoms, the value of $(E_0 - E_F)$ decreases, thereby decreasing the TEP. Consequently, in the present study, as the homogenization temperature increased, the TEP of the zirconium-based alloys decreased continuously until it reached the plateau corresponding to the solution limit.
2. The solution limit of niobium in the Zr–0.8 at.% Sn alloy could be estimated at 730 °C to be about 0.7 at.%.
3. From the investigation of the TEP evolution and optical microstructure, the transformation from α to β phase occurred in the temperature range 910–940 °C for the 0.2 at.% Nb addition. In the case of the 0.8 at.% Nb addition, the transformation temperature decreased to below 850 °C.
4. The completion of recrystallization for the 0.2 at.% Nb addition required about 60 min of aging in the temperature range of 575–600 °C, and about 10 min in the range 625–650 °C. In the case of the 0.5 at.% Nb addition, the required aging time was increased for the completion of recrystallization.

References

[1] G.P. Sabol, G.R. Kilp, M.G. Balfour, E. Roberts, in: Eighth International Symposium on Zirconium in the Nuclear Industry, vol. 1023, ASTM STP, 1989, p. 227.
[2] F. Garzarolli, H. Seidel, R. Tricot, J.P. Gros, in: Ninth International Symposium on Zirconium in the Nuclear Industry, vol. 1132, ASTM STP, 1991, p. 395.
[3] T. Isobe, Y. Matsuo, in: Ninth International Symposium on Zirconium in the Nuclear Industry, vol. 1132, ASTM STP, 1991, p. 346.
[4] A. Miquet, D. Charquet, J. Nucl. Mater. 105 (1982) 132.
[5] S.N. Tiwari, K. Tangri, J. Nucl. Mater. 34 (1970) 92.
[6] D. Arias, L. Roberti, J. Nucl. Mater. 118 (1983) 143.
[7] N.V. Korotkova, Izv. Akad. Nauk SSSR, Metally (5) (1990) 206.
[8] A. Peruzzi, J. Bolcich, J. Nucl. Mater. 174 (1990) 1.
[9] A. Peruzzi, J. Nucl. Mater. 186 (1992) 89.
[10] H. Zou, G.M. Hood, J.A. Roy, R.J. Schultz, J.A. Jackman, J. Nucl. Mater. 210 (1994) 239.
[11] A.D. Pelton, L. Leibowitz, R.A. Blomquist, J. Nucl. Mater. 201 (1993) 218.
[12] A. Peruzzi, J. Nucl. Mater. 186 (1992) 82.
[13] R. Borrelly, P. Merle, L. Adami, J. Nucl. Mater. 170 (1990) 147.
[14] K. Loucif, T. Borrelly, P. Merle, J. Nucl. Mater. 189 (1992) 34.
[15] K. Loucif, P. Merle, R. Borrelly, J. Nucl. Mater. 202 (1993) 193.
[16] K. Loucif, R. Borrelly, P. Merle, J. Nucl. Mater. 210 (1994) 84.
[17] N.J. Luiggi, Met. Mater. Trans. 28B (1997) 125.
[18] Y.H. Jeong, K.H. Kim, C. Nam, S.Y. Park, J.H. Baek, M.H. Lee, Y.H. Jung, B.K. Choi, in: Symposium on Nuclear Materials and Fuel 2000, Korea, 24–25 August, 2000, p. 655.
[19] F.J. Blatt, P.A. Schroeder, C.L. Foiles, D. Greig, Thermoelectric Power of Metals, Plenum, New York, 1976.
[20] D.D. Pollock, Physics of Engineering Materials, Prentice Hall, New Jersey, 1990.
[21] T.B. Massalski, Binary Alloy Phase Diagrams, 2nd Ed., ASM, 1990, p. 2788.